Nova Scientia
Revista de Investigación de la Universidad De La Salle Bajío

Nº 20, Vol. 10 (1), 2018. **ISSN 2007 – 0705**, pp.: 244 - 262

Assessment of cast steel anchorage fracture toughness of a cable-stayed bridge by small punch test

Evaluación de la tenacidad a la fractura de anclajes de aceros colados de un puente atirantado por ensayo miniatura de punzonamiento

E. López Vargas[1], L. A. Alcaraz Caracheo[1], J. A. Álvarez Laso[2], R. Lacalle Calderón[2], R. Rodríguez Castro[3], M. Martínez Madrid[4] y A. Sánchez Rodríguez[3]

Palabras Clave: ensayo miniatura de punzonamiento; resistencia a la fractura; aceros colados de baja aleación; puente atirantado; anclaje
Keywords: small punch test; fracture toughness; low-alloy cast steel; cable-stayed bridge; anchorage

Recepción: 02-01-2018 / Aceptación: 19-04-2018

Resumen

La evaluación de la vida residual de componentes estructurales en servicio requiere conocer el valor de la tenacidad a la fractura, pero los métodos convencionales para medir la tenacidad demandan remover grandes cantidades de material del componente, lo cual es generalmente impráctico. Sin embargo, el Ensayo Miniatura de Punzonamiento (EMP) (que utiliza especímenes miniatura no estandarizados) ha sido empleado como una alternativa práctica y conveniente para evaluar las características de fractura del material de componentes en servicio. El propósito de esta investigación fue encontrar una relación entre la deformación a la fractura equivalente de EMP ε_{af} y la tenacidad a la fractura J_{IC} de aceros colados de baja aleación procedentes de anclajes de un puente atirantado localizado en el Golfo de México. La tenacidad a la fractura J_{IC} se calculó a partir de los datos experimentales reportados de K_{IC} en un trabajo previo y la deformación a la fractura equivalente se obtuvo mediante el EMP empleando especímenes de 10x10 mm^2 por 0.5 mm de espesor. A partir de los resultados de ε_{af} y J_{IC} obtenidos, y correspondientes datos de aceros de baja aleación de la literatura, una correlación lineal fue propuesta para estimar la tenacidad de fractura a partir de la deformación a la fractura equivalente del EMP para los aceros colados pertenecientes a este caso de estudio.

[1]Depto. de Ingeniería Mecatrónica. Instituto Tecnológico de Celaya, Celaya, Guanajuato, México. E-mail: alejandro.alcaraz@itcelaya.edu.mx
[2]Depto. Ciencia e Ingeniería del Terreno. E. T. S. de Ingenieros de Caminos, Canales y Puertos. Universidad de Cantabria, Cantabria, España
[3]Depto. de Ingeniería Mecánica. Instituto Tecnológico de Celaya, Celaya, Guanajuato, México
[3]Instituto Mexicano del Transporte. Querétaro, México

Abstract

The assessment of the residual lifetime of in-service structural components requires knowledge of fracture toughness values; however, conventional test methods for measuring fracture toughness demand the removal of large material samples from components, which generally is impractical. Recently, the Small Punch Test (SPT) (which utilizes nonstandard miniature specimens) has been used as a practical and convenient alternative for evaluating fracture toughness characteristics of the material of components in service. The purpose of this research was to find a correlation between the SPT equivalent fracture strain ε_{qf} and the fracture toughness J_{IC} of low-alloy cast steels coming from anchorages of a cable-stayed bridge, which is located in the Gulf of México. Fracture toughness was calculated from K_{IC} experimental data from previous work and equivalent fracture strain ε_{qf} was obtained by SPT using specimens 10×10 mm^2 squares of 0.5 mm thickness. From ε_{qf} and J_{IC} results and corresponding low-alloy steel experimental data from literature, a linear correlation was proposed to estimate fracture toughness from SPT equivalent fracture strain for cast steels belonging to this study case.

Introduction

Fracture toughness is one of the most important material properties for assessing the structural integrity (Webster, 2000) or investigate the causes of component failures (Urriolagoitia, 2012; Dclgado, 1998). In the case of components in service, a sample of material must be removed to evaluate fracture toughness which could endanger the integrity of that component; additional concerns arise when the critical testing region is so small that specimens cannot be obtained with the minimum size requirements of the standard test methods. Consequently, test methodologies have been developed focusing on sub-sized specimens that allow significant material data to be derived from a small quantity of sample material.

In the last decades, the Small Punch Test (SPT) has proved to be a promising testing technique in assessing mechanical properties by using reduced size specimens. The SPT was initially used in mechanical property characterization of irradiated material within the nuclear industry (Manahan, 1981; Mao, 1987; Mao 1991) and later was introduced as a quasi-nondestructive method for evaluating local mechanical properties in service structural elements with large dimensions (Fleury, 1998; Viswanathan, 1994; Lacalle, 2008; Madia, 2013; Guan, 2011; Dogan, 2012; Cárdenas 2012). The small punch test basically comprises punching very small

square specimens, measuring 10×10 mm2 and 0.5 mm thickness, until fracture using a rigid ball; see Figure 1.

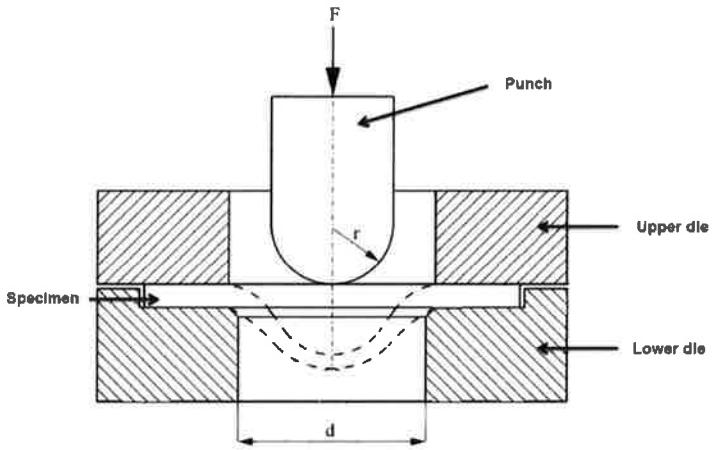

Figure 1. Small punch testing device scheme (CWA 15627, 2008).

During the test, the force–displacement curves are registered. From these curves, tensile mechanical properties have been successfully estimated (Fleury, 1998; Rodríguez, 2009; Ruan, 2002) along with fracture toughness properties (Mao 1987, Mao 1991). Several researchers (Mao, 1987; Guan, 2011; García, 2014; Mao, 1987; Misawa, 1989; Wang, 2008) have reported that there exists a linear relationship between the fracture toughness parameter J_{IC} and the SPT data, which can be expressed by Eq. 1:

$$J_{IC} = k \cdot \varepsilon_{qf} - J_0 \qquad (1)$$

Where k and J_0 are material constants, whereas ε_{af} is the equivalent fracture strain given by Eq. (2):

$$\varepsilon_{qf} = ln\left(\frac{t_0}{t_f}\right). \qquad (2)$$

In the last equation, t_0 and t_f are the initial and final thickness of the fracture specimen, respectively; see Figure 2.

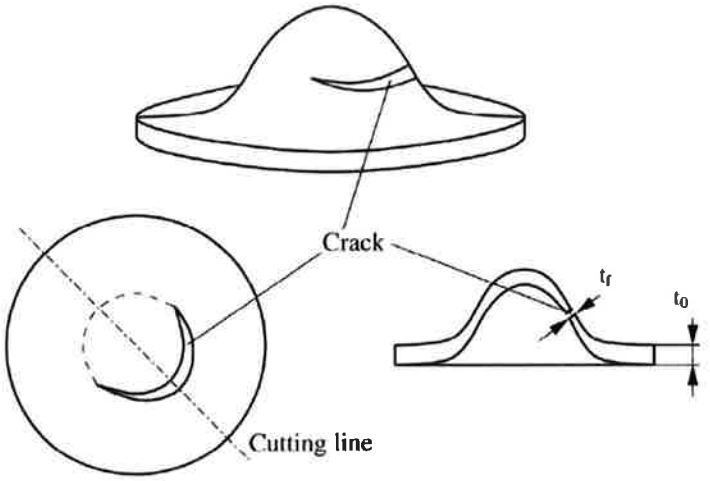

Figure 2. Initial and final thickness at fracture zone in small punch specimen (CWA 15627, 2008).

Although good correlations between fracture toughness parameters and SPT data have been found, values of the constants k and J_0 constants are distinctive for each material (García, 2015). In the case of structural steels, most of SPT studies have focused on wrought steels, while only a few investigations have concentrated on cast steels, regardless of the brittle nature of these steels. Therefore, more extensive investigation under the SPT technique is needed for cast steels.

The cast steel investigated in this work corresponds to the cable anchorages of a cable-stayed bridge that contains 112 cable anchorages; see Figure 3. One of the cable anchorages failed during normal operation in 2000 after five years of service. Since then, several scientific and engineering studies have been realized for assessment of its structural integrity. López *et al.* (2009) presented an analysis using ultrasonic and liquid penetrant techniques, and the results revealed the presence of several micro-structural defects, such as pores, cracks, inclusion and large grain size, derived from an improper fabrication condition. Alcaraz *et al.* (2012) developed research about the fracture toughness size effect on SE(B) specimens using 1Cr-½Ni cast steel, whereas Quintana *et al.* (2014) performed a damage evaluation study employing a novel method called a global search method for complex structures. Alcaraz (2012) developed a probabilistic analysis for anchorage structural integrity using probabilistic density functions of material properties and applied stress. Terán *et al.* (2014) carried out a structural integrity assessment of the anchorages using failure assessment diagrams, including the effects of residual stress and three different types of defects.

Based on an ultrasonic study (López, 2009), 16 anchorages in critical condition (large number of microstructural defects) were removed from the bridge along with four anchorages considered in "good condition" to study several properties. Two of them were used in the present research to evaluate whether the SPT could be a technique to determine the fracture toughness of the remaining in-service cast steel anchorages on the bridge.

Experimental Methods

Previous work: Mechanical characterization by standard methods (Alcaraz, 2012)

The materials under study are cast steels from two different cable anchorages (see Figure 3), where the chemical composition, microstructural details, and tensile and fracture toughness properties were determined according to current standards. The chemical composition was obtained by applying the optical spark emission technique under the ASTM E1019 and ASTM E415 standards. The microstructure characterization was performed by optical microscopy after specimen polishing and chemical attack with Nital-3%. A total of 9 rectangular specimens from anchorage 1 and 34 rectangular specimens from anchorage 2 were prepared for tensile testing according to the ASTM E8 standard. In addition, plane-strain fracture toughness K_{IC} was determined following the guidelines of the ASTM E399 standard; SE(B) three-point bend specimens were fabricated with a maximum thickness allowed by the limited dimensions of the respective anchorages. Thus, from anchorage 1, two 52-mm-thick specimens were obtained, whereas one specimen of 60 mm thickness was fabricated from anchorage 2.

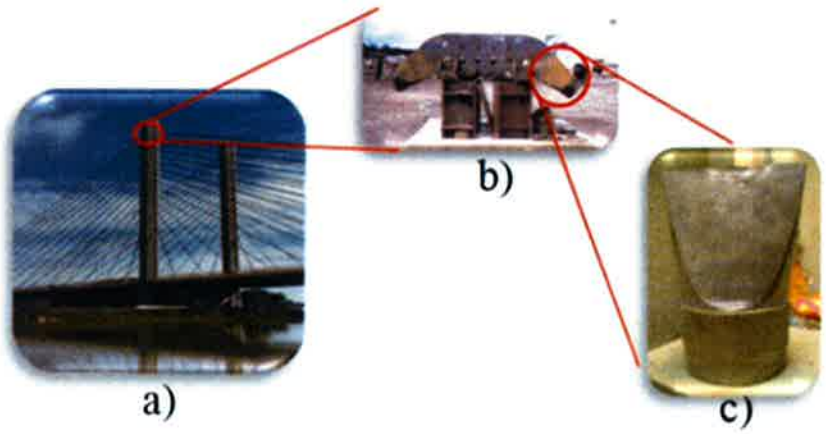

Figure 3. a) Cable-Stayed bridge on Papaloapan River, México; b) Set of anchorages welded with the tapered plate; c) Anchorage put out of service.

Small punch technique characterization

As mentioned, a widely used correlation for assessing the fracture toughness of metallic materials by means of the small punch technique is given by Eq. (1). This expression, which relates the fracture parameter J_{IC} with the equivalent fracture strain ε_{qf}, has proved to give good approximations. In fact, fitting coefficients k and J_0 for several materials have been reported by some authors (Mao, 1987; Wang, 2008; Guan, 2011). In the present work, the fitting parameters mentioned above have been used for the fracture toughness estimation of the cast steels under study, and they are shown in Table 1.

Table 1. Empirical models used for fracture toughness estimation.

Model	Reference
$J_{IC} = k \cdot \bar{\varepsilon}_{qf} - J_0$	General model
$J_{IC} = 345 \cdot \bar{\varepsilon}_{qf} - 113$	[Mao, 1987]
$J_{IC} = 370 \cdot \bar{\varepsilon}_{qf} - 40$	[Wang, 2008]
$J_{IC} = 276.77 \cdot \bar{\varepsilon}_{qf} + 0.5207$	[Guan, 2011]

Moreover, additional k and J_0 values were also obtained by using (ε_{qf}, J_{IC}) values from anchorage 2 and corresponding low-alloy steel values from literature (Guan, 2011), see Table 2, where the main alloying element was Chromium (Cr). It is worth mentioning that (ε_{qf}, J_{IC}) values from weld steels were not considered from such reference because the steel under study is a cast steel without welding. The ε_{qf} value from anchorage 2 was calculated by using Eq. (2), while J_{IC} was obtained by means of Equation (3), where E is Young's modulus and v represents Poisson's ratio of the material.

$$K_{IC} = \sqrt{\frac{E \cdot J_{IC}}{1 - v^2}} \qquad (3)$$

The small punch test specimens considered were 10×10 mm^2 squares of 0.5 mm thickness. Eigth test pieces were prepared from anchorage 1 and eigth samples from anchorage 2. The testing

machine used was a Zwick Roell single-column equipment, model BT1-FR2.5TS.140, 2500 N loading capacity. The SPT compression tests were performed at room temperature under displacement control by using TestExpert software (Zwick Roell) at a speed of 0.6 mm/min as recommended (CWA 15627, 2008).

Table 2. Set of (ε_{af}, J_{IC}) points used in correlation Eq. (1) from Guan (2011) and anchorage 2.

Material	ε_{qf}	J_{IC} **(kJ/m²)**
2.25Cr1Mo	1.1281	315.71
2.25Cr1Mo (embrittlement)	1.1452	332.28
2.25Cr1Mo weld (as received)	0.3528	110.67
2.25Cr1Mo weld (de-embrittlement)	0.9786	239.65
1.25Cr0.5Mo	0.7174	219.21
40CrNi2Mo	0.4936	117.00
25Cr2NiMo1V	0.8675	204.50
23CrNiMoWV	0.8827	282.40
0.8Cr0.6Ni (Anchorage 2)	0.2336	10.18

Results and Discussion

Mechanical characterization by standard methods

Chemical analysis results from previous work of the two cable anchorage steels are shown in Table 3. Based on their alloying elements, the materials were classified as low-alloy cast steels, where anchorage 1 is named 1Cr-0.5Ni, and anchorage 2 as 0.8Cr-0.6Ni. Figure 4 presents metallographic examinations from the two anchorages. In both cast steels, a characteristic ferrite-pearlite microstructure is observed; however, some differences can be distinguished concerning the phase distribution, possibly due to a deficient heat treatment (López, 2009). Also, some sulfides and pores are also observed (Figure 5), as well as macroscopic discontinuities (Figure 6).

Table 3. Chemical composition of the two cast steels from cable anchorages (Alcaraz, 2012).

Achorage	C	Mn	Si	S	P	Cr	Mo	Ni	Cu
1	0.423	0.820	0.803	0.022	0.034	1.007	0.093	0.537	0.343
2	0.397	0.707	0.300	0.036	0.036	0.813	0.080	0.603	0.340

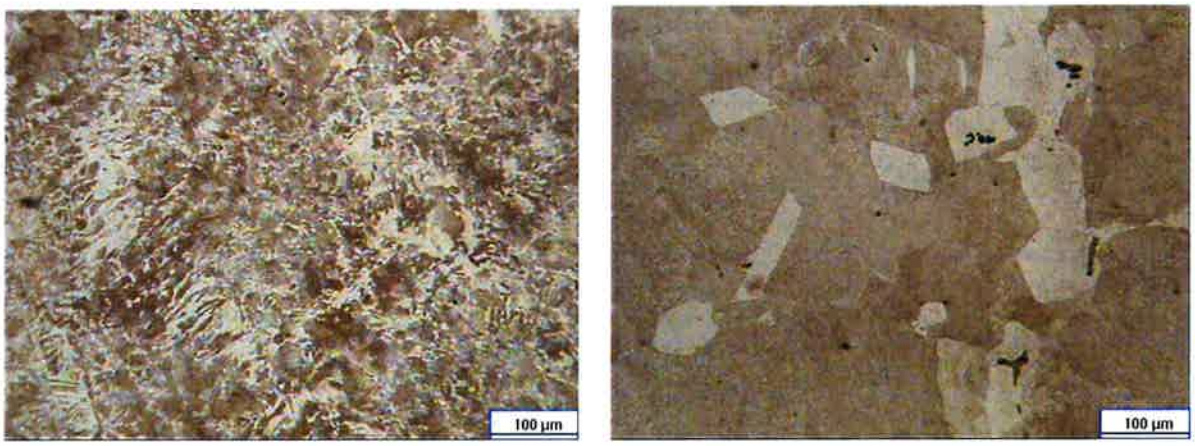

Figure 4. Microstructure in anchorage 1 (left) and anchorage 2 (right), 200X.

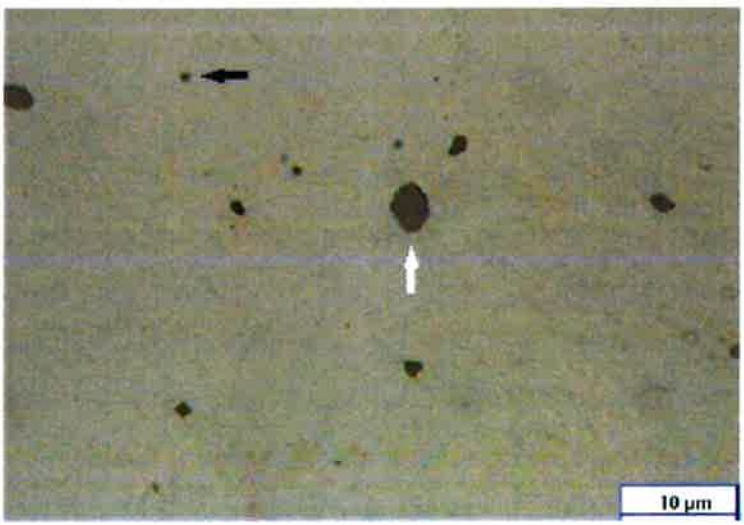

Figure 5. Sulfides (white arrow) and pores (black arrow) observed in both anchorages (Alcaraz, 2012).

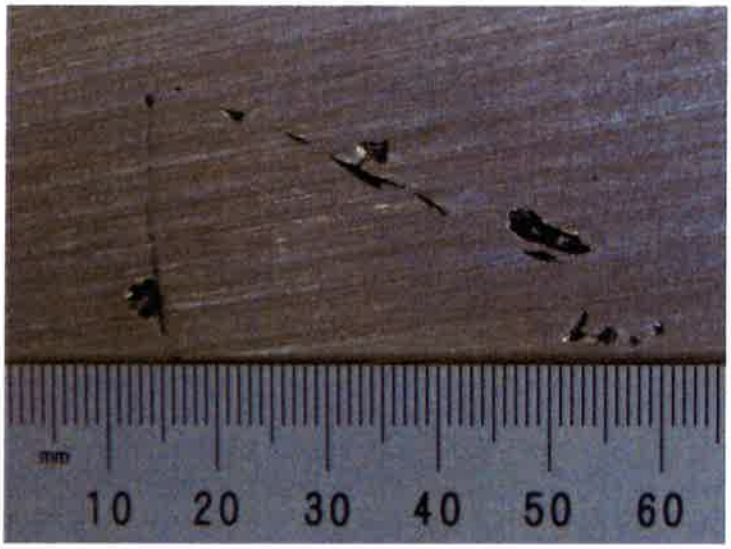

Figure 6. Macro-pores and cavities observed in both anchorages (Alcaraz, 2012).

The tensile mechanical properties obtained from previous work are shown in Table 4. It is observed that the steel from anchorage 1 has a yield and ultimate strength higher than those of anchorage 2; however, the ductility is higher for the cast steel from anchorage 2, as evidenced by the elongation percent. Figure 7 shows stress–strain curves for the two cast steels for comparison purposes. The stress–strain curve from anchorage 1 is typical of high-resistance steel, whereas the corresponding curve for anchorage 2 is representative of high-ductility steels with extensive plastic strain prior to fracture.

Table 4. Tensile properties of the two cast steels from cable anchorages (Alcaraz, 2012).

Anchorage	***E*** **(GPa)**	***S_y*** **(MPa)**	***S_u*** **(MPa)**	***Elongation*** **(%)**
1	199	323	621	8.4
2	195	280	591	12.6

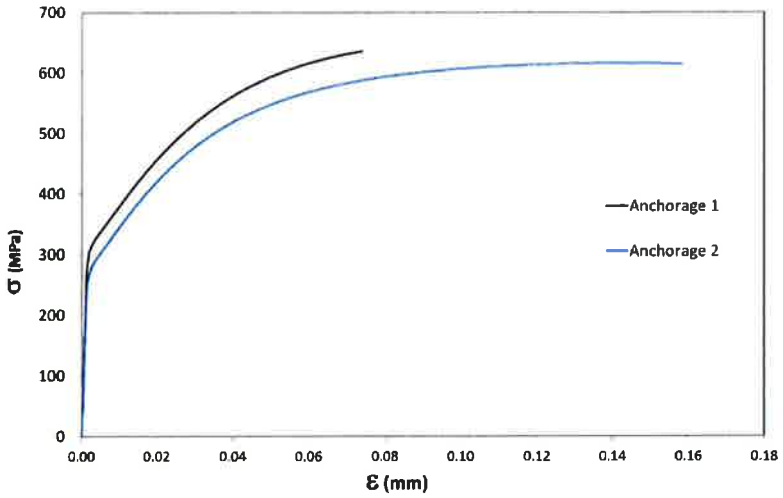

Figure 7. Stress–strain curves for both anchorages.

The fracture toughness testing results according to ASTM E399 standard are shown in Table 5. By comparing fracture toughness K_{IC} values for both anchorages, anchorage 2 presents a higher value than anchorage 1. The difference can be explained by the high ductility exhibited by anchorage 2 with respect to anchorage 1; see Table 4.

Table 5. Fracture toughness K_{IC} for anchorages 1 and 2 (Alcaraz, 2012).

Anchorage	Thickness mm	K_{IC} MPa·m$^{1/2}$
1	52	39.4
2	60	47.5

Small Punch Test Characterization

Load–displacement curves obtained from small punch testing for both anchorages are shown in Figure 8. These curves display a characteristic ductile behavior for both steels (Lacalle, 2012). Some clear differences can be appreciated between both curve sets if the maximum values of load and displacement are considered. The set of curves for anchorage 1 exhibits lower load and displacement values than the corresponding values for anchorage 2. According to this result, the SPT technique yields load–displacement curves with good repeatability and thus can make a

capable distinction between the two types of cast steels; nevertheless, the maximum load values slightly fluctuate. This last behavior is linked to local strain concentrations arising before the maximum load is reached, leading to material instabilities (Lacalle, 2012).

The failure morphology displayed by the small punch specimens for both anchorages showed a hemispherical surface, and fracture occurred along the circumference where the strain is highest; see Figure 9. This failure mode is typical of ductile steels.

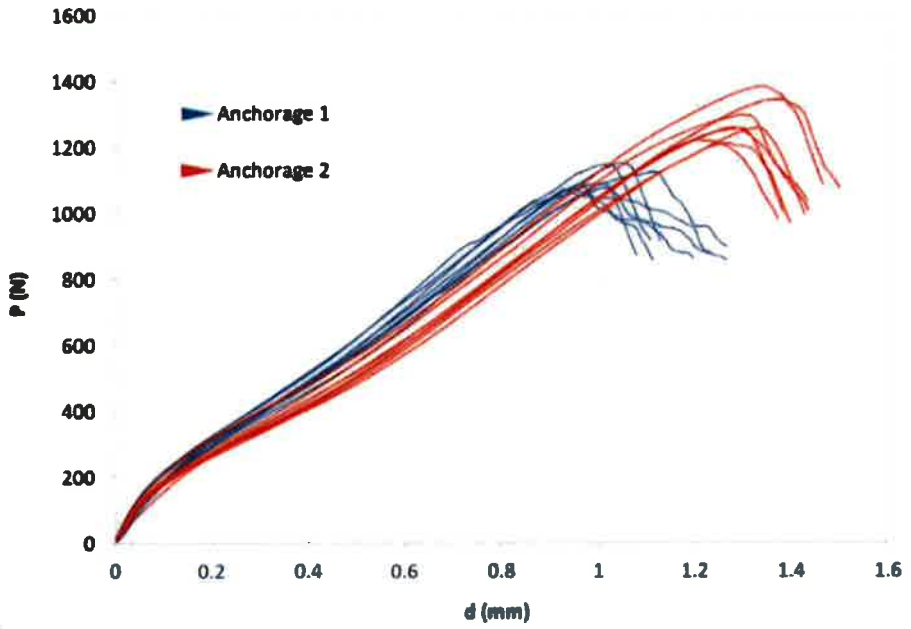

Figure 8. SPT load–displacement curves for steel specimens in anchorage 1 (left) and anchorage 2 (right).

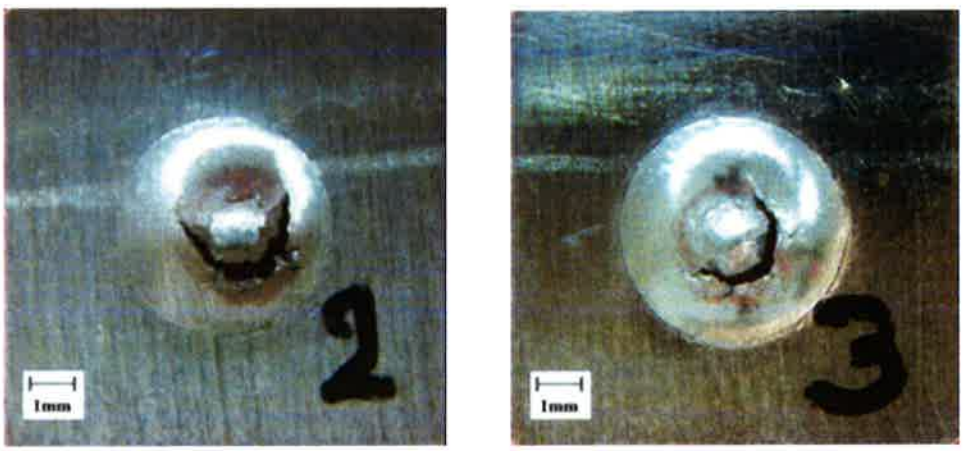

Figure 9. Fracture morphology in small punch specimens in anchorage 1 (left) and anchorage 2 (right).

To analyze the SPT fracture toughness results, the equivalent fracture strain ε_{qf} is used. This parameter is calculated from a modified version of Eq. (2) (Mao, 1987), which is given as

$$\varepsilon_{qf} = 0.09\left(\frac{d*}{t_0}\right) \qquad (4)$$

Where d* is the displacement at fracture, which is obtained from the load–displacement curves for the fractured specimens. Thus, d* and ε_{qf} values for the specimens from anchorages 1 and 2 are shown in Table 6. By observing the displacement values d* from both anchorages, it is then clear that the cast steel from anchorage 2 shows higher ductility, as previously concluded from Figure 8 and Table 4.

Table 6. d* and ε_{af} parameters for anchorage 1 (left) and anchorage 2 (right).

Specimen	d^* mm	ε_{qf}	Specimen	d^* mm	ε_{qf}
1	1.05	0.19	1	1.20	0.22
2	1.12	0.20	2	1.30	0.23
3	0.97	0.17	3	1.28	0.23
4	1.02	0.18	4	1.29	0.23
5	1.02	0.18	5	1.34	0.24
6	0.93	0.17	6	1.33	0.24
7	1.00	0.18	7	1.27	0.23
8	0.95	0.17	8	1.37	0.25
Average	1.01	0.18	**Average**	1.30	0.23

Table 7 shows the results obtained when the equivalent fracture strain, ε_{qf} (Table 6), is introduced into the different correlation models given in Table 1. Corresponding K_{IC} values are obtained by using Eq. (3) and compared with the K_{IC} value found from the standard fracture mechanics technique (ASTM E399, 2004). It is observed that the K_{IC} values from empirical relationships (Wang, 2008; Guan, 2011) support once again the higher toughness of anchorage 2. However, by comparing such values with the K_{IC} reference value obtained from the standard ASTM E399 technique, the SPT K_{IC} values are more than 60% higher. On the other hand, when the parameters are substituted into the relationship proposed (Mao, 1987) for the materials under study, negative K_{IC} values are obtained, which have no physical meaning. This difference can be attributed to materials used in correlations since coefficients can be different. In addition, specimen thickness and device dimensions have an important effect on the results. In fact, this is one of the reasons why the European Committee for Standardization (CWA 15627, 2008) recommends unifying these parameters.

Table 7. SPT fracture toughness results for anchorage 1 (left) and anchorage 2 (right).

Model	K_{IC} ($MPa \cdot m^{1/2}$) Anchorage 1	K_{IC} ($MPa \cdot m^{1/2}$) Anchorage 2
[Wang, 2008]	76.62	99.72
[Guan, 2011]	105.17	118.18
[ASTM E399, 2004]	39.4	47.18

To achieve better estimates of the fracture toughness values for the cast steels under study, k and J_0 values were obtained by using an additional correlation with (ε_{qf}, J_{IC}) values (Guan, 2011), along with corresponding values from anchorage 2; see Table 2. Figure 10 shows a J_{IC}–ε_{qf} plot from such data, along with the trend line with fitting parameters k=340.27 and J_0=54.19 and correlation coefficient R^2=0.9511. Thus, the new empirical relationship results in Eq. (5).

$$J_{IC} = 340.27 \cdot \bar{\varepsilon}_{qf} - 54.19 \qquad (5)$$

This new correlation was tested by substituting the ε_{qf} value from anchorage 1 to obtain a new K_{IC} value, which is 40.87 MPa·m$^{1/2}$. A better approximation was reached, with 4% error compared to previous models. Thus, for the anchorage cast steels under study, the empirical model (5) is proposed for fracture toughness assessment by the small punch technique.

Finally, Figures 11 (obtained from previous work) and 12 show fractographs from standard and small punch tested specimens, respectively. The fracture surface from the standard specimen shows trans-granular cleavage with ductile tearing, which is associated with a triaxial stress state (Alcaraz, 2012). In contrast, the fracture surface from the SPT specimen exhibits ductile tearing with a considerable quantity of micro-voids. This type of fracture can be associated with a biaxial stress state (insignificant third stress component), which yields extensive plastic deformation throughout the reduced thickness of the SPT specimen.

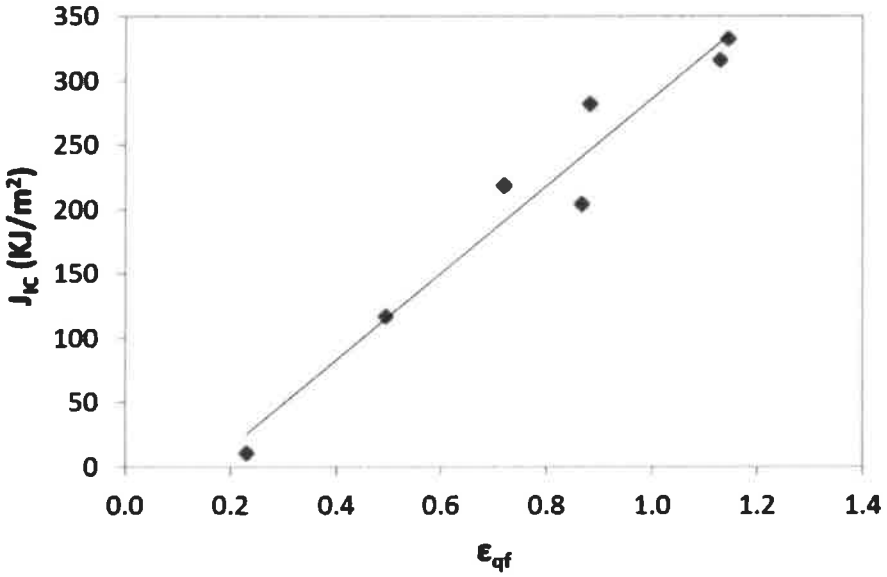

Figure 10. Equivalent fracture strain ε_{af}–fracture toughness J_{IC} correlation.

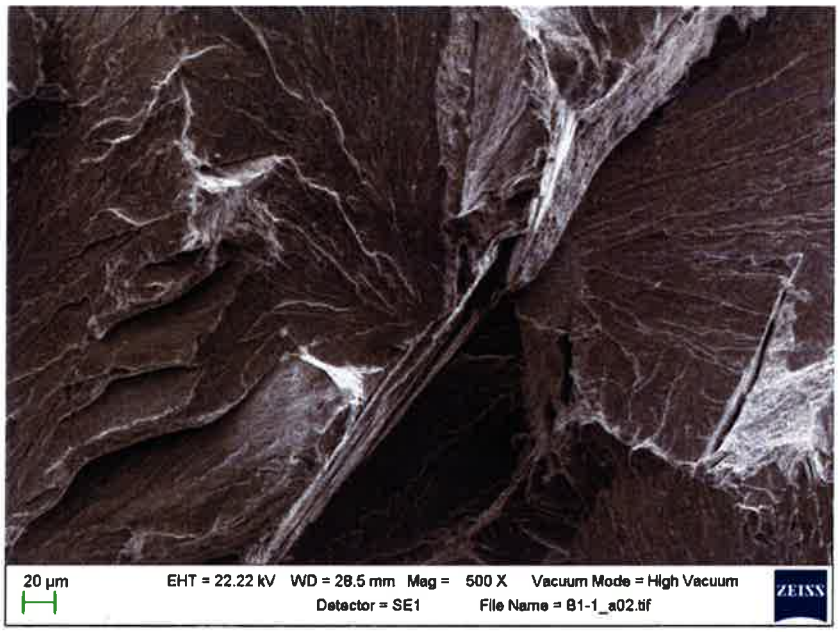

Figure 11. Fractograph for a standard specimen showing cleavage behavior plus dimples and tear ridges (Alcaraz, 2012).

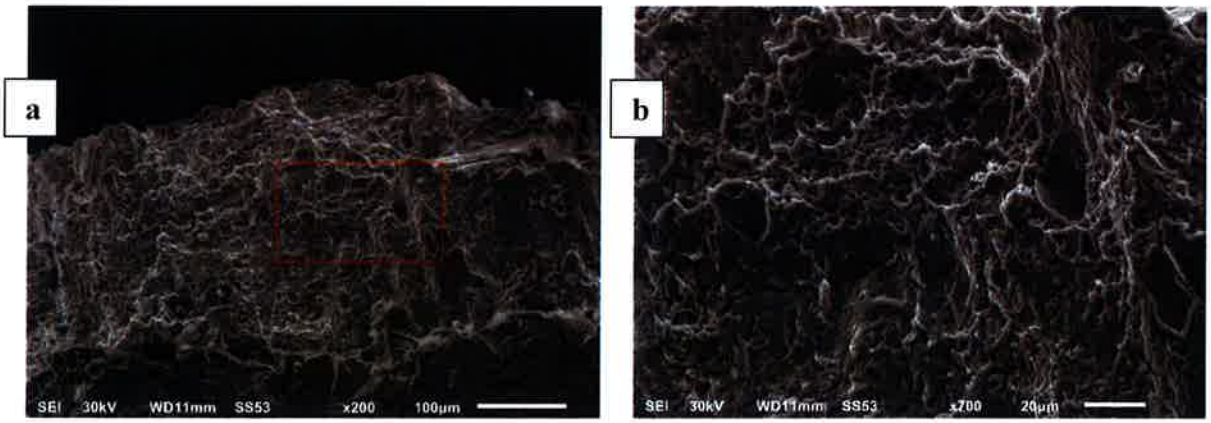

Figure 12. Typical fractograph for SPT specimens: (a) through-thickness fracture, (b) Detail of the rectangule in (a) exhibites ductile failure by micro-void growth and coalescence.

Conclusions

This work involved a comparative analysis of fracture toughness results from standard specimen tests and from small punch rests for low-alloy Cr-Ni cast steels coming from the anchorages of a cable-stayed bridge. Empirical correlations reported in the literature show that fracture toughness values obtained from the SPT technique are not good approximations in comparison with the ASTM E399 standard. This discrepancy can be attributed to materials used in correlations and due

to specimen and device dimensions. In this way, for the cast steels under study, new fitting parameters of the used model were proposed for SPT fracture toughness assessment. The results showed a good linear correlation between fracture toughness and equivalent fracture strain, R^2=0.9511, where the empirical fitting parameters were k=340.27 and J_0=54.19. This correlation demonstrated a good capability for estimating the fracture toughness of cast steel anchorages of the bridge under study, and these findings show considerable promise for its application as a quasi-nondestructive fracture toughness technique for remaining life assessment of in-service anchorages of bridges. Fractographic analysis showed size specimen dependence on the fracture mechanism; small punch specimens showed ductile fracture, whereas standard samples showed quasi-cleavage fracture mode.

References

Alcaraz-Caracheo L. A. (2012). Análisis probabilístico de integridad de un anclaje de acero estructural (Tesis Doctoral). Retrieve from: http://www.sepi.esimez.ipn.mx/posgradomecanica/tesis/2010/analisisprobabilistico.pdf. Escuela Superior de Ingeniería Mecánica y Eléctrica, Sección de Estudios de Posgrado e Investigación, Instituto Politécnico Nacional, México.

Alcaraz-Caracheo, L.A., Terán-Guillén, J., Carrión-Viramontes, F.J. & Martínez-Madrid, M. (2012). Correlation between Specimen Size and Fracture Toughness of 1Cr-½Ni Cast Steel Used in the Anchorage of a Cable-Stayed Bridge. *Científica. 16(3)*, 135-143. Retrieve from: http://www.redalyc.org/articulo.oa?id=61426384004.

ASTM E 1019-03 (2004). Test Methods for Determination of Carbon, Sulfur, Nitrogen, and Oxygen in Steel and in Iron, Nickel, and Cobalt Alloys, ASTM International, PA, USA.

ASTM E 415-99A (2004) Test Method for Optical Emission Vacuum Spectrometric Analysis of Carbon and Low-Alloy Steel, ASTM International, PA, USA.

ASTM E 8. (2004). Standard Test Method for Tension Testing of Metallic Materials, ASTM International, West Conshohocken, PA, USA.

ASTM E399. (2004). Standard Test Method for Plain-Strain Fracture Toughness of Metallic Materials, ASTM International, West Conshohocken, PA, USA.

Cárdenas, E., Belzunce, F. J., Rodriguez, C., Penuelas, I. & Betegón, C. (2012). Application of the small punch test to determine the fracture toughness of metallic materials. *Fatigue &*

Fracture of Engineering Materials & Structures, 35(5), 441-450. DOI: 10.1111/j.1460-2695.2011.01635.x

CWA 15627. (2008). Small Punch Test for Metallic Materials, CEN Workshop Agreement, European Committee for Standardization.

Dogan, B. & Hyde, T. (2012). Industrial application of Small Punch Testing for in-service component condition assessment: An overview. ASME 2012 *Pressure Vessels and Piping Conference*. (6): 1003-1010. Ontario, Canada

Delgado, H. & Hernández, H. (1998). Estudio metalúrgico de causas de falla del puente pescadero. *Ingeniería e Investigación*, *39*, 12-28. Retrieve from: http://www.revistas.unal.edu.co/index.php/ingeinv/article/view/20973

Fleury, E. & Ha, J.S. (1998). Small punch tests to estimate the mechanical properties of steels for steam power plant: I. Mechanical strength. *International Journal of Pressure Vessels and Piping*, 75(9), 699-706. DOI: 10.1016/S0308-0161(98)00074-X.

García, T.E., Rodríguez, C., Belzunce, F.J. & Cuesta, I.I. (2015). Development of a new methodology for estimating the CTOD of structural steels using the small punch test. *Engineering Failure Analysis, (50)*, 88-99. DOI: 10.1016/j.engfailanal.2015.01.011.

García, T.E., Rodríguez, C., Belzunce, F.J. & Suárez, C. (2014). Estimation of the mechanical properties of metallic materials by means of the small punch test. *Journal of Alloys and Compounds*, *(582)*, 708-717. DOI: 10.1016/.jallcom.2013.08.009.

Guan, K., Hua, L., Wang, Q., Zou, X. & Song, M. (2011). Assessment of toughness in long term service CrMo low alloy steel by fracture toughness and small punch test. *Nuclear Engineering and Design*, *241(5)*, 1407-1413. DOI: http://dx.doi.org/10.1016/j.nucengdes.2011.01.031.

Lacalle, R. (2012). *Determinación de las propiedades en tracción y fractura de materiales metálicos mediante ensayos Small Punch*. (Tesis Doctoral). Universidad de Cantabria, España.

Lacalle, R., Álvarez, J. A., & Gutiérrez-Solana, F. (2008). Analysis of key factors for the interpretation of small punch test results. *Fatigue & Fracture of Engineering Materials & Structures*, *31*(10), 841-849. DOI: 10.1111/j.1460-2695.2008.01262.x

López, J.A., Carrión, F.J., Quintana, J.A., Samayoa-Ochoa, D., Lomelí, M.G. & Orozco, P.R. (2009). Verification of the Ultrasonic Qualification for Structural Integrity of Partially

Concrete Embedded Steel Elements. *In Advanced Materials Research, (65)*, 69-78. DOI: 10.4028/www.scientific.net/AMR.65.69.

Madia, M., Foletti, S., Torsello, G. & Cammi, A. (2013). On the applicability of the small punch test to the characterization of the 1CrMoV aged steel: Mechanical testing and numerical anal-ysis. *Engineering Failure Analysis, (34)*, 189-203. DOI: 10.1016/j.engfailanal.2013.07.028.

Manahan, M.P., Argon, A.S. & Harling, O.K. (1981). The development of a miniaturized disk bend test for the determination of post-irradiation mechanical properties. *Journal of Nuclear Materials, (104)*, 1545-1550. DOI: 10.1016/0022-3115(82)90820-0.

Mao, X., Shoji, T. & Takahashi, H. (1987). Characterization of fracture behaviour in small punch test by combined recrystallization-etch method and rigid plastic analysis. *Journal of Testing and Evaluation, 15(1)*, 30-37. DOI: 10.1520/JTE11549J.

Mao, X. & Takahashi, H. (1987). Development of a further-miniaturized specimen of 3 mm diameter for tem disk (ø 3 mm) small punch tests. *Journal of Nuclear Materials, 150(1)*, 42-52. DOI: 10.1016/0022-3115(87)90092-4.

Mao, X., Takahashi, H. & Kodaira, T. (1991). Estimation of mechanical properties of irradiated nuclear pressure vessel steel by use of sub-sized CT specimen and small punch specimen. *Scripta metallurgica et materialia, 25(11)*, 2487-2490. DOI: 10.1016/0956-716X(91)90054-5.

Misawa, T., Nagata, S., Aoki, N., Ishizaka, J. & Hamaguchi, Y. (1989). Fracture toughness evaluation of fusion reactor structural steels at low temperatures by small punch tests. *Journal of Nuclear Materials, (169)*, 225-232. DOI: 10.1016/0022-3115(89)90538-2.

Quintana, J., Carrión, F. & Crespo, S. (2014). Damage detection on a cable stayed bridge using wave propagation analysis. *7th European Workshop on Structural Health Monitoring*, Nantes, France.

Rodríguez, C., Cabezas, J.G., Cárdenas, E., Belzunce, F. J. & Betegón, C. (2009). Mechanical properties characterization of heat-affected zone using the small punch test. *Welding journal, 88(9)*, 188-192. Retrieved from: https://app.aws.org/wj/supplement/wj0909-188.pdf.

Ruan, Y., Spätig, P. & Victoria, M. (2002). Assessment of mechanical properties of the martensitic steel EUROFER97 by means of punch tests. *Journal of nuclear materials, (307)*, 236-239. DOI: 10.1016/S0022-3115(02)01194-7.

Terán, J., Cicero, S., García, T., Alvarez, J.A., Martínez, M., Pérez, J.T. (2014). Structural integrity assessment of the cast Steel upper anchorage elements used in a cable stayed bridge. *Engineering structures, (81)*, 309-317. DOI: 10.1016/j.engstruct.2014.10.018.

Urriolagoitia-Sosa, G., Urriolagoitia-Calderon, G., Romero-Ángeles, B., Torres-Franco, D., Hernández-Gómez, H., Molina-Ballinas, A., Torres-San Miguel, C.R., Campos-López, J.P. (2012). Using fracture mechanics for determining residual stres fields in diverse geometries. *Ingeniería e Investigación, 32(3)*, 19-26. Retrieve from: www.revistas.unal.edu.co/index.php/ingeinv/article/view/35935.

Viswanathan, R. (1994). Small punch testing for determining the material toughness of low alloy steel components in service. *Journal of Engineering Materials and Technology, (116)*, 457-464. DOI: 10.1115/1.2904313.

Wang, Z.X., Shi, H.J., Lu, J., Shi, P. & Ma, X.F. (2008). Small punch testing for assessing the fracture properties of the reactor vessel steel with different thicknesses. *Nuclear engineering and design, 238 (12)*, 3186-3193. DOI: 10.1016/j.nucengdes.2008.07.013.

Webster, S. & Bannister, A. (2000). Structural integrity assessment procedure for Europe–of the SINTAP programme overview. *Engineering Fracture Mechanics, 67(6)*, 481-514. DOI: 10.1016/S0013-7944(00)00070-9.